

A whole-body mathematical model of cholesterol metabolism and transport

Peter Emil Carstensen^{*,**} Jacob Bendtsen^{*,**}
Laura Hjort Blicher^{*,**} Kim Kristensen^{**}
John Bagterp Jørgensen^{*}

^{*} Technical University of Denmark, Department of Applied
Mathematics and Computer Science, DK-2800 Kgs. Lyngby, Denmark
^{**} Novo Nordisk A/S, DK-2880 Bagsværd, Denmark

Abstract: Cardiovascular diseases are the leading cause of death. Increased levels of plasma cholesterol are consistently associated with an increased risk of cardiovascular disease. As a result, it is imperative that studies are conducted to determine the best course of action to reduce whole-body cholesterol levels. A whole-body mathematical model for cholesterol metabolism and transport is proposed. The model can simulate the effects of lipid-lowering drugs like statins and anti-PCSK9. The model is based on ordinary differential equations and kinetic functions. It has been validated against literature data. It offers a versatile platform for designing personalized interventions for cardiovascular health management.

Keywords: Mathematical modeling, Metabolism, Systems biology, Multi-scale modeling, Quantitative Systems Pharmacology (QSP), Cholesterol, Cardiovascular disease, Obesity

1. INTRODUCTION

The human body has several metabolic processes that continuously produces and uses cholesterol to maintain homeostasis. Cholesterol molecules are transported in lipoproteins and used in the cell for synthesis of hormones and vitamins as well as for cell membrane formation. Lipoproteins also have a vital function in supplying cells with free fatty acids for storage in the adipose tissue. Disruption in the lipoproteins homeostasis can lead to various diseases including atherosclerosis (cholesterol deposits in the blood vessel walls). Atherosclerosis can happen due to prolonged high cholesterol concentration in plasma. This cholesterol formation may rupture and lead to a clot in the legs, the lungs, or the brain. This can cease blood flow and potentially be lethal (Miesfeld and McEvoy, 2017).

The development and application of physiologically based pharmacokinetic (PBPK) models in chemical toxicology has grown steadily since their emergence in the 1980s. Whole-body mathematical models are useful to describe the biological interplay between cellular regulation and convective transport between organs through the blood stream. Such models allows for simulation of concentrations in organs, the transport rate across the membrane, and the cellular reactions (Paalvast et al., 2015). Mathematical whole-body models allow for *in-silico* investigation of clinical trials prior *in-vivo* conduction of these trials. Potentially, this can accelerate the development of novel drugs and therapeutic intervention strategies.

In the early 1900s, cholesterol was discovered to be a component in atherosclerosis. In the last couple of decades,

several computational models of cholesterol metabolism and transport have been proposed. Paalvast et al. (2015) evaluated computational models of cholesterol metabolism in order to elucidate the regulation of intracellular cholesterol. Zhang et al. (2022) reviewed several in-silico models of cholesterol metabolism and transport from the gene level to the overall transport in plasma. Most of the mathematical models reviewed could not provide the needed reliable integrated multi-scale description of organ metabolism and transport between organs. The models were often unable to reproduce experimental data and predict the outcome of a drug treatment (Paalvast et al., 2015). Pratt et al. (2015) formulated a model of hepatic lipid metabolism and Toroghi et al. (2019); Sokolov et al. (2019) considered mathematical models for cholesterol metabolism with drug induced effects from statins and anti-PCSK9.

A whole-body model of the human metabolism and transport of cholesterol, with the most relevant organs, herein a meal model and a pharmacokinetic model is proposed. The results of the simulations are compared to published clinical studies from Peradze et al. (2019); Matikainen et al. (2019); Aoki et al. (2020); Taskinen et al. (2021); Mok et al. (2023). The model provides a multi-scale mathematical model, that incorporates mass balances and genetic influences, through the use of ordinary differential equations and kinetic functions. Our model approach is systematic and compact, which enables efficient representation of large metabolic networks, as well as examination of the parameters most sensitive to changes. Our mathematical model serves as an in-silico tool that captures the dynamics of cholesterol metabolism under various metabolic and drug treatment conditions. Carstensen et al. (2022) provide the whole-body model building methodology, while

^{*} Peter Emil Carstensen is at submission time funded by the The Novo Nordisk Foundation Center for Biosustainability, Technical University of Denmark, NNF20CC0035580.

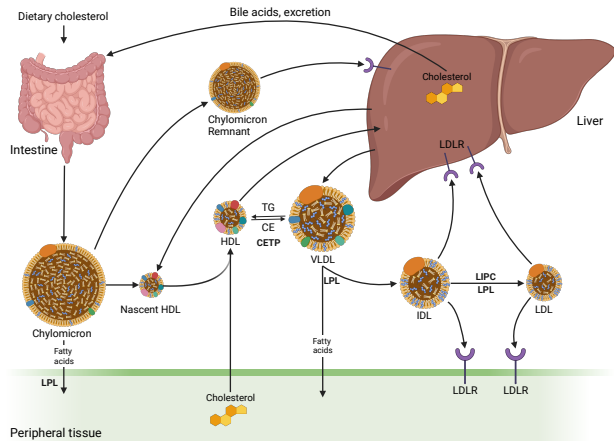


Fig. 1. Lipoprotein metabolism. Triglyceride-rich particles are secreted from the intestine (Chylomicrons) or the liver (VLDL). Chylomicrons and VLDL particles undergo lipolysis in the circulation, which yields fatty acids to peripheral tissues. Remnants are taken up by the liver. IDL is taken up by the LDLR or further metabolized to LDL. HDL is formed in circulation from lipid-poor particles (nascent HDL), that are secreted from the liver or Chylomicrons. HDL carries cholesterol from peripheral tissues to the liver or exchanges cholesterol esters and triglycerides with lipoproteins in circulation. Adapted from Lusis and Pajukanta (2008) and created with BioRender.com.

Bendsen and Carstensen (2024) provide the specific details of the cholesterol metabolism model summarized in this paper.

The remaining part of this paper is structured as follows. Section 2 describes the cholesterol metabolism and transport. Section 3 presents the mathematical model and Section 4 shows the simulation results. Section 5 discusses the results and Section 6 briefly concludes.

2. CHOLESTEROL METABOLISM AND TRANSPORT

Figure 1 shows the transport of cholesterol throughout the human body and the interplay of different lipoproteins (VLDL, IDL, LDL, Chylomicron, Remnant). Cholesterol is transported in the body via lipoproteins. Dietary lipids are absorbed and packed into Chylomicrons. Chylomicrons consist of cholesterol, phospholipids, and free fatty acids (FFA). Lipoprotein lipases (LPL) release these FFA to peripheral tissues. The Chylomicron Remnants (Chylomicron without FFA) binds to receptors in the liver. Non-dietary cholesterol is transported from the liver to tissues in very low density lipoproteins (VLDL). VLDL are metabolized by LPL into intermediate density lipoprotein (IDL), which can be further metabolized into low density lipoprotein (LDL). IDL and LDL binds to receptors in various tissues for degradation into cellular cholesterol. High density lipoprotein (HDL) removes excess cholesterol from peripheral tissues. Through the cholesteryl ester transfer protein (CETP), HDL can also exchange triglycerides and cholesteryl esters with other lipoproteins. Cholesterol is regulated at a cellular level by sterol regulatory element-binding protein 2 (SREBP-2). SREBP-2 is inhibited by

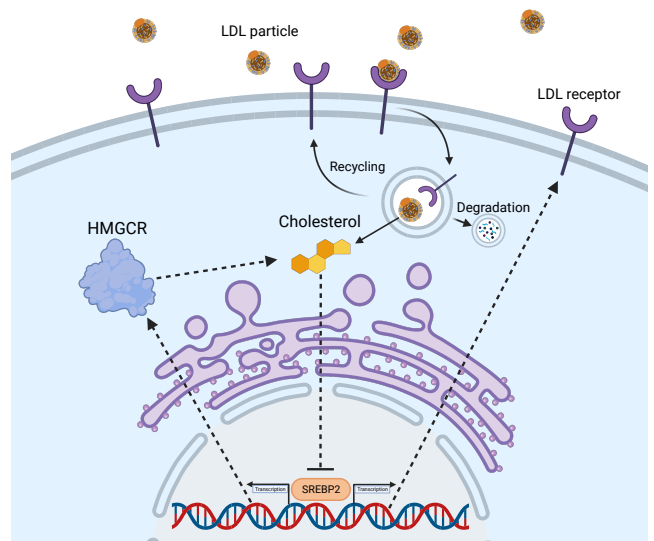


Fig. 2. Cellular regulation of cholesterol and the LDLR. SREBP-2 binds to the HMGCR gene to produce HMGCR, that stimulates cholesterol synthesis. SREBP-2 also binds to the LDLR gene to produce LDLR. High cholesterol concentrations inhibit SREBP-2. LDL particles bind to LDLR in the interstitial space and the LDLR-LDL complex is internalized. If PCSK9 is bound to the LDLR, the receptor is degraded, otherwise it can be recycled to the surface. Created with BioRender.com.

high cholesterol concentrations, as illustrated in Figure 2 (Miesfeld and McEvoy, 2017).

Liraglutide is a GLP-1 receptor agonist, used for the treatment of type 2 diabetes, and chronic obesity (ref). Liraglutide also reduces the risk of cardiovascular disease (CVD) by reducing the cholesterol levels (Peradze et al., 2019; Matikainen et al., 2019; Taskinen et al., 2021). According to Peradze et al. (2019), the cholesterol concentration levels are reduced with daily injections of 3.0 mg Liraglutide. This dose only has minor impact on cholesterol concentration in HDL, VLDL, and IDL. Taskinen et al. (2021) describe that Liraglutide can lead to reduced Chylomicron and VLDL concentrations. In turn they lead to decreased Remnant formation. Figure 3 shows the proposed mechanism of Liraglutide on dietary cholesterol intake (Taskinen et al., 2021). Liraglutide has a direct suppressive action on ApoB48 synthesis in the gut. Liraglutide reduces the postprandial production rate of Chylomicron-ApoB48 by 60%. As a consequence of the reduced ApoB48 availability, the Chylomicrons assemble themselves in larger particles. The larger Chylomicron particles can be lipolysed more rapidly than the smaller Chylomicron particles and have a reduced direct clearance. Taskinen et al. (2021) also compare blood samples before and after treatment with Liraglutide. They observe a smaller concentration of ApoB48 containing particles in treatments with Liraglutide. This is also supported by previous experiments (Matikainen et al., 2019). Additionally, the reported data in Taskinen et al. (2021) show a reduction in the accumulation of liver fat. The VLDL secretion rate scales with the amount of liver fat. Therefore, less liver fat means less VLDL secretion (Taskinen et al., 2021).

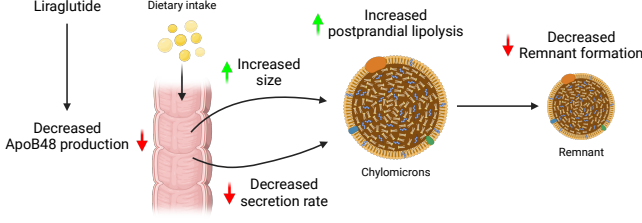


Fig. 3. Proposed mechanism of action of Liraglutide on dietary intake and Chylomicrons. Liraglutide decreases (red arrow) ApoB48 production, leading to increased (green arrow) size of Chylomicrons and increased postprandial lipolysis. A decreased secretion due to fewer ApoB48 particles reduces the amount of Chylomicrons and leads to reduced Remnant formation. Adapted from Taskinen et al. (2021) and created with BioRender.

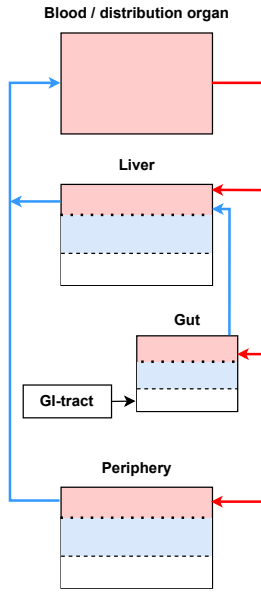


Fig. 4. The cholesterol flow model. The Periphery should be perceived as a lumped compartment. Dietary cholesterol is absorbed in the gut cellular space.

3. MODEL

The model in this paper is a connected system with four organs: Blood (B), Liver (L), Gut (G), and Periphery (P). Periphery is a lumped compartment of all other organs. Figure 4 shows the connected system. The GI-tract refers to a meal uptake model (Ritschel et al., 2023). Figure 5 illustrates the additional division of organs into Vascular, Interstitial and Cellular. Figure 5 is denoted the organ model.

Consider the set of organs, $\mathcal{O} = \{B, L, G, P\}$. Then the mass balances for the vascular part is

$$V_{Ov}\dot{C}_{Ov} = q_O - C_{Ov}Q_{O,out} + f_{Ov} \quad \forall O \in \mathcal{O} \quad (1a)$$

$$q_O = \sum_{\bar{O} \in \mathcal{I}_O} C_{\bar{O}v}Q_{\bar{O}} \quad \forall O \in \mathcal{O} \quad (1b)$$

$$Q_{O,out} = \sum_{\bar{O} \in \mathcal{I}_O} Q_{\bar{O}} \quad \forall O \in \mathcal{O} \quad (1c)$$

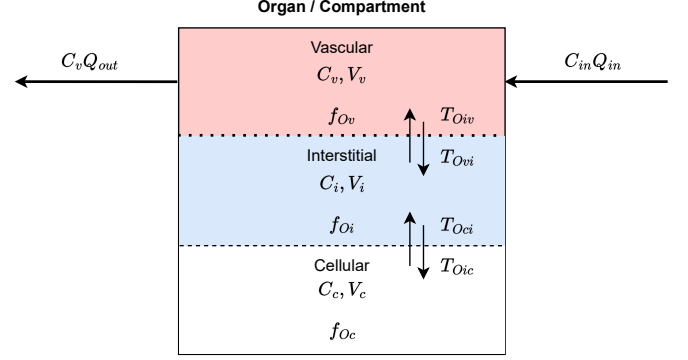


Fig. 5. The organ model with 3 compartments: Vascular, Interstitial, Cellular. The metabolism in each compartment is described by f_O , the transport between compartments is defined by T_O and the blood flow between organs is defined by $C \cdot Q$.

The mass balances for the interstitial organ spaces and the cellular organ spaces can be described as

$$V_{Oi}\dot{C}_{Oi} = f_{Oi} \quad \forall O \in \mathcal{O} \setminus \{B\} \quad (2a)$$

$$V_{Oc}\dot{C}_{Oc} = f_{Oc} \quad \forall O \in \mathcal{O} \setminus \{B\} \quad (2b)$$

V_{Ov} , V_{Oi} and V_{Oc} the vascular, interstitial and cellular volumes respectively. \mathcal{I}_O is the set of inflows to organ O . f_{Ov} , f_{Oi} and f_{Oc} are the vascular, interstitial and cellular transport and reaction rates and can be expressed as

$$f_{Ov} = -T_{Ovi}V_{Ov} + T_{Oiv}V_{Oi} + R_{Ov}V_{Ov} \quad (3a)$$

$$f_{Oi} = T_{Ovi}V_{Ov} - T_{Oiv}V_{Oi} - T_{Oic}V_{Oi} + T_{Oci}V_{Oc} + R_{Oi}V_{Oi} \quad (3b)$$

$$f_{Oc} = T_{Oic}V_{Oi} - T_{Oci}V_{Oc} + R_{Oc}V_{Oc} + s_{Oc} \quad (3c)$$

Transport between compartments occurs through a concentration gradient and is expressed as

$$T_{Ovi} = k_{Ovi}C_{Ov} \quad \forall O \in \mathcal{O} \setminus \{B\} \quad (4a)$$

$$T_{Oiv} = k_{Oiv}C_{Oi} \quad \forall O \in \mathcal{O} \setminus \{B\} \quad (4b)$$

$$T_{Oic} = k_{Oic}C_{Oi} \quad \forall O \in \mathcal{O} \setminus \{B\} \quad (4c)$$

$$T_{Oci} = k_{Oci}C_{Oc} \quad \forall O \in \mathcal{O} \setminus \{B\} \quad (4d)$$

The production rates in each compartment

$$R_{Ov} = \nu'_{Ov}r_{Ov}(C_{Ov}) \quad \forall O \in \mathcal{O} \quad (5a)$$

$$R_{Oi} = \nu'_{Oi}r_{Oi}(C_{Oi}) \quad \forall O \in \mathcal{O} \setminus \{B\} \quad (5b)$$

$$R_{Oc} = \nu'_{Oc}r_{Oc}(C_{Oc}) \quad \forall O \in \mathcal{O} \setminus \{B\} \quad (5c)$$

are obtained from the stoichiometry, ν , and reaction rates, $r(C)$, whose kinetics depend on the current concentration of the species for each compartment in all organs \mathcal{O} .

The term s_{Oc} represents a sink or source function within the cellular space. A source could provide the intestines with dietary cholesterol and a sink could be the conversion of cholesterol to bile in the liver.

3.1 Reactions

Figure 6 shows the reactions and transport that occur within the liver. VLDL and Remnant particle transport only occurs in the liver. The biochemical reaction model for cholesterol is the same in the Liver, the Gut, and the Periphery. The transport varies from organ to organ, where the transport is greater in the Liver. The Gut secretes dietary Chylomicrons and the Periphery secretes excess cellular cholesterol to circulating HDL particles.

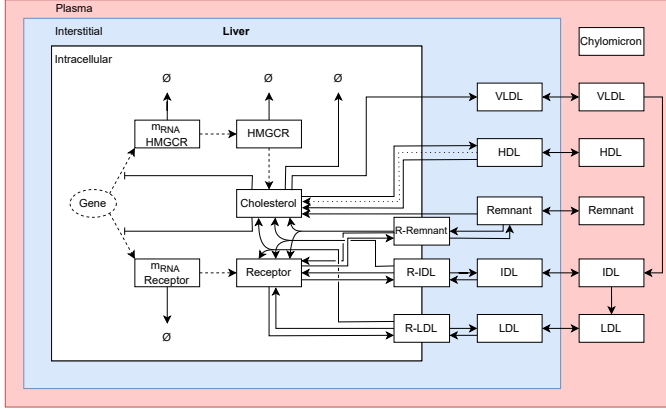


Fig. 6. The cholesterol metabolism in the liver. The white area is the intracellular space, the blue area is the interstitial space, and the red area is the vascular space. The solid arrows represent mass transfer, the dashed arrows represent transfer of cholesterol molecules, the blunt arrows represent inhibition, the bidirectional arrows represent diffusion, and the dashed circle represents the nucleus of the cell.

3.2 Liraglutide pharmacokinetic-pharmacodynamic model

The pharmacokinetics of Liraglutide is simulated by a slightly modified model in Watson et al. (2010), i.e. a one compartment model with first order absorption and first order elimination.

$$\dot{A}_1 = u(t) - K_A A_1 \quad (6a)$$

$$V \dot{D}_1 = K_A A_1 - CL D_1 \quad (6b)$$

$u(t)$ is the dosing rate of Liraglutide, K_A is the absorption constant, A_1 is the amount of Liraglutide in the absorption compartment. V is the distribution volume of Liraglutide, CL is the clearance, and D_1 is the concentration of Liraglutide in the distribution compartment (Watson et al., 2010). The pharmacodynamics, i.e. the effect, of Liraglutide (D_1) on Chylomicrons is implemented as activation of lipolysis and inhibition of secretion. It is assumed that all organs has the Liraglutide concentration D_1 .

4. RESULTS

4.1 Liraglutide

Liraglutide dosing is simulated as an incremental dosing regimen. The doses are: 0.6 mg/day in week 1; 1.2 mg/day in week 2; 1.8 mg/day in the subsequent weeks. Figure 7 shows a simulated 24 week Liraglutide therapy. The simulated relative reduction compares well with experimental data from the literature (Peradze et al., 2019; Matikainen et al., 2019; Aoki et al., 2020; Taskinen et al., 2021; Mok et al., 2023). The simulated therapy results in a 10% LDL cholesterol (LDL-c) reduction after 24 weeks.

4.2 Statins

Figure 8 shows simulations of statin therapy for different diets. The effect of statins are simulated by inhibition of the endogenous production of cholesterol by 85% (Paalvast

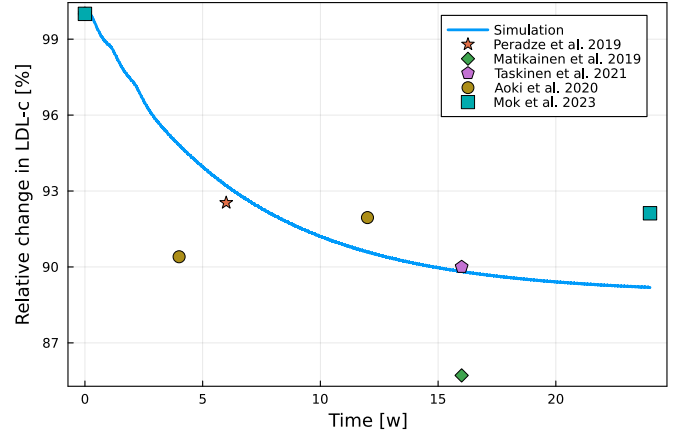


Fig. 7. Relative drop in LDL-c after 24 weeks treatment with incremental increases in dose until 1.8 mg/day Liraglutide. The data points are digitized data.

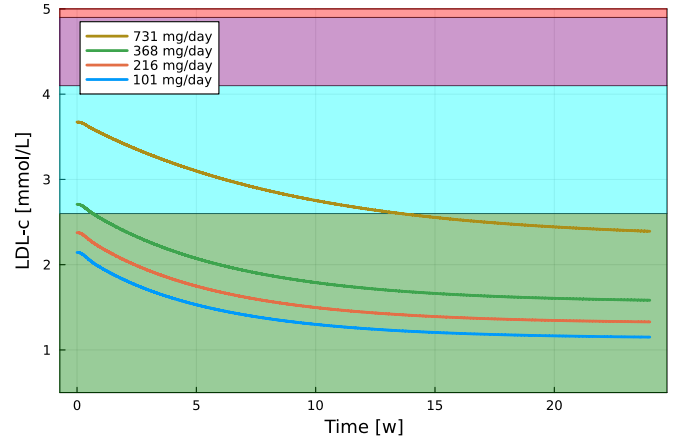


Fig. 8. The simulated LDL-c for persons in statin treatment over 24 weeks with different diets (cholesterol intake per day). Red: Very high, Purple: High, Cyan: Borderline high, and Green: Optimal (Cleeman, 2001).

et al., 2015). Figure 8 show a simulation of LDL-c reduction in a person treated with a statin therapy over 24 weeks combined with different dietary cholesterol intake.

4.3 Anti-PCSK9

Figure 9 shows simulations based on anti-PCSK9 therapy over 24 weeks. The effect of anti-PCSK9 is modelled as a decreased receptor degradation (Bendsen and Carstensen, 2024). The after-treatment steady-states vary according to dietary cholesterol intakes. The largest simulated cholesterol intake results in a LDL-c steady-state of 1.31 mmol/L (64% reduction). The smallest simulated dietary cholesterol intake results in a steady-state of 1.01 mmol/L (53% reduction). Hence, in anti-PCSK9 treatment, the dietary intake of cholesterol on the final LDL-c level is small.

4.4 Statins and anti-PCSK9

In a study by McKenney et al. (2012), the effects of anti-PCSK9 was investigated in patients who had already been

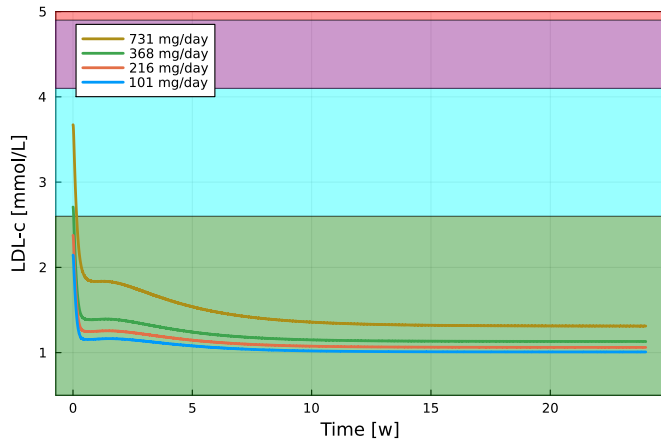


Fig. 9. The simulated LDL-c for persons in anti-PCSK9 treatment over 24 weeks with different diets (cholesterol intake per day). Red: Very high, Purple: High, Cyan: Borderline high, and Green: Optimal (Cleeman, 2001).

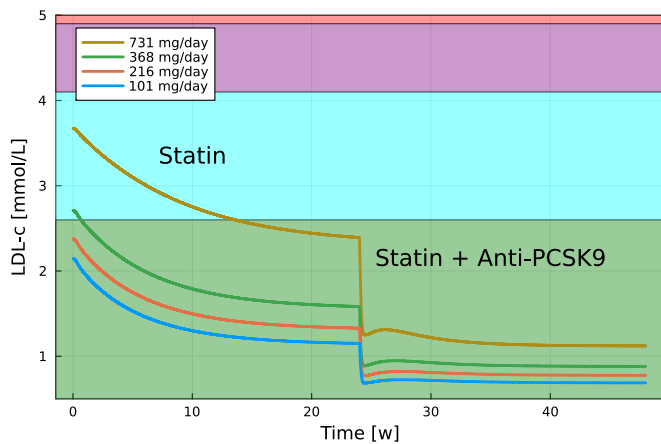


Fig. 10. Simulated LDL-c for different diets (cholesterol intakes) in a therapy with 24 weeks of statin dosing followed by 24 weeks of combined statin and anti-PCSK9 dosing. Red: Very high, Purple: High, Cyan: Borderline high, and Green: Optimal (Cleeman, 2001).

on statin treatment for a period greater than six weeks. McKenney et al. (2012) show that the LDL-c could be further reduced by 40-72%. This is simulated by a 24 week period of treatment with statins and then additional 24 weeks of statin and anti-PCSK9 treatment. Figure 10 shows simulated results similar to the results by McKenney et al. (2012).

4.5 Sensitivity analysis

A sensitivity analysis is performed for all parameters related to metabolism and transport. This is done by separately doubling or halving all parameter values in relation to their nominal value and simulating of the model for 52 weeks. Figure 11 shows the effect on LDL-c for each of the 50 parameters in the model. Twenty parameters are identified to have a significant effect on the LDL-c concentrations. The parameter $k_{VLDL\ sec}$ (parameter 13) increases the total amount of lipoproteins in the

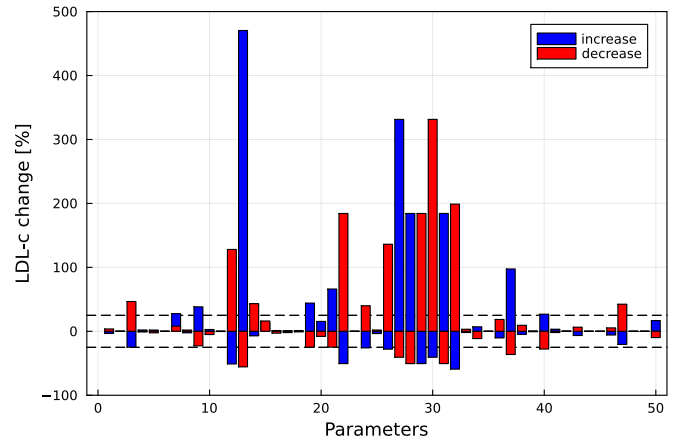


Fig. 11. Bar plot of the result of the global sensitivity analysis. Doubling parameter value: *increase* (blue), halving parameter value: *decrease* (red). The dashed lines indicate the cutoff of $\pm 25\%$ change in LDL-c concentrations at steady state.

bloodstream and leads to the highest increase in LDL-c. The parameter δ_c (parameter 32) is related to the degradation rate of cholesterol in the liver. This parameter leads to the largest reduction in the LDL-c concentration. The model is sensitive to the biosynthesis of cholesterol, as 5 of the 20 most significant parameters are associated with the endogenous production of cholesterol. The parameter associated with receptor-recycling has a high influence on the LDL-c concentration. Increasing this parameter mimics the effect of anti-PCSK9.

5. DISCUSSION

Statins and anti-PCSK9 impact different parameters within the model. Simulations shows that the proposed model is capable of incorporating these drugs. Statins vary in strength for their reduction of cholesterol. Statins can provide 20-50% reduction in LDL-c (Scharnagl et al., 2001). The simulated statin therapy showed a reduction of 35-47% for the four different cholesterol intakes. Anti-PCSK9 therapy reduces cholesterol levels from 40-70% (Lambert et al., 2012). The simulated anti-PCSK9 treatment shows a 53-64% reduction in LDL-c. The model's analysis of therapeutic interventions with the combination of statins and anti-PCSK9 treatments, shows an additional 41-63% reduction in LDL-c. This is also within the 40-72% additional reduction reported by McKenney et al. (2012).

The sensitivity analysis shows that most of the significant parameters are already targets of current lipid lowering drugs. Two new possible targets have been identified. If a drug can inhibit the secretion rate of VLDL, our model shows a significant impact on the LDL-c concentration. If a drug can increase the degradation rate of cholesterol then our model also shows significant reduction in LDL-c. Inhibition of VLDL secretion will inevitably increase the cellular cholesterol concentration. Given an increased cellular cholesterol, the degradation rate of cholesterol becomes highly relevant. A drug that targets both, would be effective in lowering the lipid composition. Further validation of the model is required to determine if this is a valid drug target.

6. CONCLUSION

We provide a whole-body mathematical model of the cholesterol metabolism in man. The model can be used to simulate LDL-c lowering therapies with Liraglutide, statins, anti-PCSK9 and combinations of statins and anti-PCSK9. A model sensitivity analysis demonstrates that the biosynthesis of cholesterol is important. The model and the simulations indicate that *in-silico* clinical test may be a valuable supplement to guide *in-vivo* clinical trials. In addition, the model and the modeling activity provide an advanced understanding of cholesterol metabolism and transport. The corresponding insights enable further research and refinement of mathematical models for dynamical simulation of cholesterol metabolism and possible therapies. Future work may extend the model with individual population metrics (allometric scaling) to design personalized intervention strategies for cardiovascular health.

REFERENCES

- Aoki, K., Kamiyama, H., Takihata, M., Taguri, M., Shibata, E., Shinoda, K., Yoshii, T., Nakajima, S., and Terauchi, Y. (2020). Effect of liraglutide on lipids in patients with type 2 diabetes: a pilot study. *Endocrine Journal*, 67(9), 957–962.
- Bendsen, J. and Carstensen, P.E. (2024). *Combination of Quantitative Systems Pharmacology (QSP) and Physiology Based Pharmacokinetic Models (PBPK) for Simulation of the Cholesterol Metabolism in Man*. Master’s thesis, Technical University of Denmark. Department of Applied Mathematics and Computer Science.
- Carstensen, P.E., Bendsen, J., Reenberg, A.T., Ritschel, T.K.S., and Jørgensen, J.B. (2022). A whole-body multi-scale mathematical model for dynamic simulation of the metabolism in man. *IFAC PapersOnLine*, 55(23), 58–63.
- Cleeman, J.I. (2001). Executive summary of the third report of the national cholesterol education program (NCEP) expert panel on detection, evaluation, and treatment of high blood cholesterol in adults (adult treatment panel III). *JAMA*, 285(19), 2486–2497.
- Lambert, G., Sjouke, B., Choque, B., Kastelein, J.J.P., and Hovingh, G.K. (2012). The PCSK9 decade: Thematic review series: New lipid and lipoprotein targets for the treatment of cardiometabolic diseases. *Journal of Lipid Research*, 53(12), 2515–2524.
- Lusis, A.J. and Pajukanta, P. (2008). A treasure trove for lipoprotein biology. *Nature Genetics*, 40(2), 129–130.
- Matikainen, N., Söderlund, S., Björnson, E., Pietiläinen, K., Hakkarainen, A., Lundbom, N., Taskinen, M., and Borén, J. (2019). Liraglutide treatment improves postprandial lipid metabolism and cardiometabolic risk factors in humans with adequately controlled type 2 diabetes: A single-centre randomized controlled study. *Diabetes, Obesity and Metabolism*, 21(1), 84–94.
- McKenney, J.M., Koren, M.J., Kereiakes, D.J., Hanotin, C., Ferrand, A.C., and Stein, E.A. (2012). Safety and efficacy of a monoclonal antibody to proprotein convertase subtilisin/kexin type 9 serine protease, SAR236553/REGN727, in patients with primary hypercholesterolemia receiving ongoing stable atorvastatin therapy. *Journal of the American College of Cardiology*, 59(25), 2344–2353.
- Miesfeld, R.L. and McEvoy, M.M. (2017). *Biochemistry*. W.W. Norton & Company.
- Mok, J., Adeleke, M.O., Brown, A., Magee, C.G., Firman, C., Makahamadze, C., Jassil, F.C., Marvasti, P., Carnemolla, A., Devalia, K., Fakih, N., Elkalaawy, M., Pucci, A., Jenkinson, A., Adamo, M., Omar, R.Z., Batterham, R.L., and Makaronidis, J. (2023). Safety and efficacy of liraglutide, 3.0 mg, once daily vs placebo in patients with poor weight loss following metabolic surgery: The bari-optimize randomized clinical trial. *Jama Surgery*, 158(10), 1003–1011.
- Paalvast, Y., Kuivenhoven, J.A., and Groen, A.K. (2015). Evaluating computational models of cholesterol metabolism. *Biochimica Et Biophysica Acta - Molecular and Cell Biology of Lipids*, 1851(10), 1360–1376.
- Peradze, N., Farr, O.M., Perakakis, N., Lázaro, I., Sala-Vila, A., and Mantzoros, C.S. (2019). Short-term treatment with high dose liraglutide improves lipid and lipoprotein profile and changes hormonal mediators of lipid metabolism in obese patients with no overt type 2 diabetes mellitus: A randomized, placebo-controlled, cross-over, double-blind clinical trial. *Cardiovascular Diabetology*, 18(1), 141.
- Pratt, A.C., Wattis, J.A., and Salter, A.M. (2015). Mathematical modelling of hepatic lipid metabolism. *Mathematical Biosciences*, 262, 167–181.
- Ritschel, T.K.S., Reenberg, A.T., Carstensen, P.E., Bendsen, J., and Jørgensen, J.B. (2023). Mathematical meal models for simulation of human metabolism. *arXiv:2307.16444v1*.
- Scharnagl, H., Schinker, R., Gierens, H., Nauck, M., Wieland, H., and März, W. (2001). Effect of atorvastatin, simvastatin, and lovastatin on the metabolism of cholesterol and triacylglycerides in HepG2 cells. *Biochemical Pharmacology*, 62(11), 1545–1555.
- Sokolov, V., Helmlinger, G., Nilsson, C., Zhudenkov, K., Skrtic, S., Hamrén, B., Peskov, K., Hurt-Camejo, E., and Jansson-Löfmark, R. (2019). Comparative quantitative systems pharmacology modeling of anti-pcsk9 therapeutic modalities in hypercholesterolemia. *Journal of Lipid Research*, 60(9), 1610–1621.
- Taskinen, M.R., Björnson, E., Matikainen, N., Söderlund, S., Pietiläinen, K.H., Ainola, M., Hakkarainen, A., Lundbom, N., Fuchs, J., Thorsell, A., Andersson, L., Adiels, M., Packard, C.J., and Borén, J. (2021). Effects of liraglutide on the metabolism of triglyceride-rich lipoproteins in type 2 diabetes. *Diabetes, Obesity and Metabolism*, 23(5), 1191–1201.
- Toroghi, M.K., Cluett, W.R., and Mahadevan, R. (2019). A multi-scale model for low-density lipoprotein cholesterol (LDL-C) regulation in the human body: Application to quantitative systems pharmacology. *Computers and Chemical Engineering*, 130, 106507.
- Watson, E., Jonker, D.M., Jacobsen, L.V., and Ingwersen, S.H. (2010). Population pharmacokinetics of liraglutide, a once-daily human glucagon-like peptide-1 analog, in healthy volunteers and subjects with type 2 diabetes, and comparison to twice-daily exenatide. *Journal of Clinical Pharmacology*, 50(8), 886–894.
- Zhang, F., Macshane, B., Searcy, R., and Huang, Z. (2022). Mathematical models for cholesterol metabolism and transport. *Processes*, 10(1), 155.